

Risk-Constrained Interactive Safety under Behavior Uncertainty for Autonomous Driving

Julian Bernhard¹ and Alois Knoll²

Abstract—Balancing safety and efficiency when planning in dense traffic is challenging. Interactive behavior planners incorporate prediction uncertainty and interactivity inherent to these traffic situations. Yet, their use of single-objective optimality impedes interpretability of the resulting safety goal. Safety envelopes which restrict the allowed planning region yield interpretable safety under the presence of behavior uncertainty, yet, they sacrifice efficiency in dense traffic due to conservative driving. Studies show that humans balance safety and efficiency in dense traffic by *accepting a probabilistic risk* of violating the safety envelope. In this work, we adopt this safety objective for interactive planning. Specifically, we formalize this safety objective, present the Risk-Constrained Robust Stochastic Bayesian Game modeling interactive decisions satisfying a maximum risk of violating a safety envelope under uncertainty of other traffic participants' behavior and solve it using our variant of Multi-Agent Monte Carlo Tree Search. We demonstrate in simulation that our approach outperforms baseline approaches, and by reaching the specified violation risk level over driven simulation time, provides an interpretable and tunable safety objective for interactive planning.

I. INTRODUCTION

Behavior planners for autonomous vehicles must be able to solve dense driving situations in close interaction with humans thereby being confronted with a variety of behavioral variations and limited knowledge about the true human driving behavior.

Interactive behavior planners became more and more advanced to plan in such situations. Popular approaches to predict other participants use cooperative [1–3] or probabilistic models [4, 5]. The authors presented a behavior space approach in [6] to deal with the variety of human behavior variations in interactive planning. Yet, existing approaches leave open how to specify a meaningful safety objective under the presence of behavior uncertainty. They use single-objective optimality criteria which are not interpretable with respect to a meaningful safety goal, e.g. a maximum collision probability P_{col} .

Restricting the ego motion to stay within a safety envelope, e.g. defined using reachability analysis [7–9] or other forms of safe distance measures [10, 11] circumvents the problem of prediction model inaccuracy. However, since interactions are neglected, this approach becomes problematic in crowded traffic where it leads to conservative driving or the freezing vehicle symptom.

¹Julian Bernhard is with fortiss GmbH, An-Institut Technische Universität München, Munich, Germany

²Alois Knoll is with Chair of Robotics, Artificial Intelligence and Real-time Systems, Technische Universität München, Munich, Germany

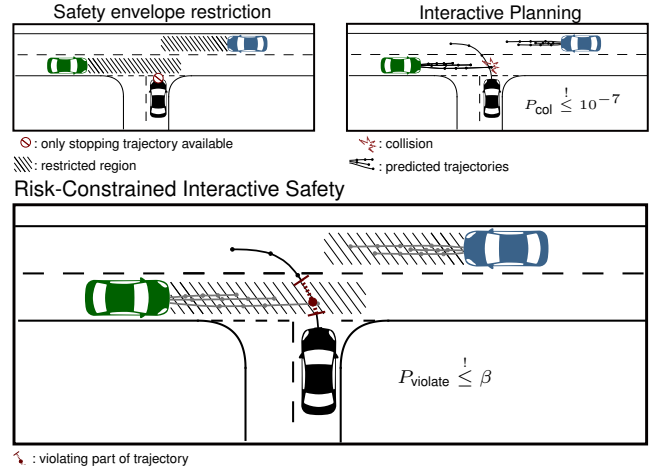


Fig. 1: Restricting the ego motion to stay within a safety envelope fosters the freezing vehicle symptom in dense traffic scenarios. Objective functions of interactive planners employable in dense traffic are not interpretable with respect to the collision probability P_{col} . Therefore, we transfer a human-related safety objective for dense traffic to interactive planning. Our planner generates a policy which satisfies a specified maximum risk level of violating a safety envelope β .

It seems that humans follow a different safety goal than realized by existing behavior planners. Evaluation over real-world driving data showed that humans violate safe distance measures with a certain percentage *averaged over driven time* [12] with increasing violations occurring in dense traffic during rush hours [13]. It seems that the safety objective of human drivers balances safety and efficiency in a comprehensible way.

In this work, we therefore adopt this safety objective for interactive planning. Our approach generates a policy which satisfies a maximum risk of violating a safety envelope under uncertainty of other traffic participants' behavior. Specifically, we contribute

- a formalization of this safety objective,
- the Risk-Constrained Robust Stochastic Bayesian Game (RC-RSBG) modeling risk-constrained interactive decisions under behavior uncertainty,
- a Multi-Agent Monte Carlo Tree Search (MA-MCTS) planner to solve the RC-RSBG,
- a simulative analysis showing that our approach outperforms baseline approaches while reaching the specified violation risk level averaged over driven time.

Fig. 1 visualizes our contribution. We start with related work. Next, we formalize the problem and present our method followed by the experimental evaluation.

II. RELATED WORK

We present related work on risk metrics and levels, interactive and risk-constrained planning.

A. Risk-metrics and levels

There exist probabilistic and non-probabilistic risk definitions. The latter defines a metric and an accompanying risk threshold. Data-related metrics use human driving data to parameterize distance functions, e.g. to fit Gaussian metrics [11] or human safety corridors from feedback in simulation [14]. Kinematics-based metrics model physics-based risk, e.g. time-to-collision [15] or potential fields to model braking forces [16] and are closely related to safety envelope definitions [10, 11] whereby a kinematic risk level of zero corresponds to completely staying within the safety envelope. Non-probabilistic risk is straightforward to define and interpret. Yet, it does not reveal information about the probability of occurrence of a harmful event and neglects uncertainty information, e.g. beliefs about the behavior of other participants.

In the functional safety sense, risk is probabilistic and defined as the combination of probability of occurrence of harm and the severity of that harm [17]. Existing probabilistic risk definitions often consider collision as harmful events in risk-based planning approaches [9, 17–19] using the state probability, the probability of spatial overlap at discrete times [20]. Value-based probabilistic risk definitions arose in finance and are applied to robotics and autonomous driving [21–23]. Defining risk based on collisions is infeasible considering the vast amount of samples required to approximate human collision probabilities $P_{col} \approx 10^{-7}$. In contrast to previous work, we propose a notion of risk coupled to how human drivers might balance safety and efficiency in interactive situations based on the risk of violating a safety envelope. By formalizing risk as event probability, with the harmful event occurring over a period of time [20], correspondence between *specified risk level and observed risk* is achieved.

B. Interactive Planning

In [24], Bernhard *et al.* define the behavior of an autonomous vehicle as *its desired future* sequence of physical states encoding the agent’s strategy to reach a short-term goal, e.g. changing lane. A behavior planner creates a behavior trajectory and passes it to a controller. In this work, we focus on modeling of risk induced by unknown behaviors of other traffic participants and drop localization and execution uncertainties. Interactive planning algorithms incorporate potential reactions of other participants into their plan to successfully navigate in congested traffic [25]. We briefly summarize existing approaches to predict other participants behavior within an interactive planning process.

Cooperative approaches assume that participants act according to a global cost function in a Multi-Agent Markov Decision Process (MA-MDP) [1–3] and allow for explainable parameterization of the model. However, the assumption that traffic follows a globally optimal solution neglects the uncertainty inherent to human interactions. *Markov approaches*

represent participants’ behavior via environment transitions based on the current observable state in a Markov Decision Process (MDP) [22, 26]. Though, MDPs model uncertainty in state transitions, they neglect information from past states, facilitating inefficient and unsafe decisions. In contrast, *Belief-based approaches* use observations from past states to gather information about the true behavior of other participants, modeled as Partially Observable Markov Decision Process (POMDP) [4, 5, 27, 28] or Bayesian game [6] to improve efficiency in dense traffic scenarios.

Existing interactive planners employ a *single-objective* optimality criterion with manual or data-based cost tuning to avoid collisions [1–5, 22, 27]. Compared to previous work, we employ a *multi-objective* optimality criterion to model risk over behavior uncertainty. For this, we combine our decision model, the Robust Stochastic Bayesian Game (RSBG) presented in [6] with the Cost-Constrained Partially Observable Markov Decision Process (CC-POMDP) [29, 30].

C. Risk-Constrained Planning

Planning under non-probabilistic risk definitions equals finding an ego trajectory within the space spanned by risk metric and level, e.g. by using graph search on a discretized state space [11] or Model Predictive Control (MPC) [31]. Probabilistic collision risk is used in [23] to model lane changing as conditional value at risk MDP, in [18] to model on ramp merging as CC-POMDP and in [17] to incorporate various uncertainties into an MPC algorithm. Related to our risk definition, Müller *et al.* [32] constrain the risk of violating the safe distance. Prescribed related work in risk-constrained planning employs long-term, i.e. maneuver-based prediction of other participants neglecting interactions. Interactive risk-constrained planning using reinforcement learning has been investigated in [22] using conditional value at risk, and in [26] using a discretized state space.

The presented approaches allow for specification of a risk constraint, yet, reveal missing correspondence between *specified and observed risk* in the experimental evaluation. In this work, we demonstrate that with our variant of MA-MCTS the observed risk in simulation corresponds to the specified constraint yielding an interpretable and tunable safety objective for interactive planning.

III. PROBLEM FORMULATION

Evaluation over real-world driving data showed that humans violate safe distance measures with a certain percentage [12, 13]. It seems that humans

- 1) **stay within** their safety envelope, e.g. spanned by the current safe distance, *in most cases* to avoid unsafe behavior due to modeling uncertainty, yet
- 2) **accept the risk*** of violating the safety envelope. They behave such that a safety envelope is violated with not more than probability β under consideration of prediction uncertainty.

*Modeling severity of envelope violations is considered future work.

By adjusting β humans tune safety versus efficiency to avoid conservative driving in congested, rush hour traffic [13]. Based on these considerations, we informally define a human-related safety objective for interactive behavior planning as: "The ego vehicle behaves such that the percentage of time the safety envelope is violated is smaller than a given threshold". Next, we formalize this safety goal.

We model the traffic environment in a game-theoretic manner [33]. It consists of N_j other agents, i.e. traffic participants, each observing a joint environment state $o^t = (o_1^t, o_2^t, \dots, o_N^t) \in \mathcal{O}$ with *physical* dynamic and static properties, e.g. participant positions and velocities, map information etc. Agents choose next actions based on their policy $a_j^t \sim \pi_j(a_j^t | o^t, \textcircled{2})$ defined over a continuous action space A_j , e.g. a 2-dimensional space bounding maximum longitudinal acceleration and steering angle. We control a single agent i , the autonomous vehicle, which selects actions from a discrete set of actions A_i according to $a_i \sim \pi_i$. It reasons about the behavior of the other agents j . Agent i knows the action space and can observe past actions of the other agents. The true policy π_j and hidden inputs $\textcircled{2}$ are *unknown* to i . Deterministic transitions to the next environment state, $o^{t+1} = T(o^t, a^t)$, result from the agents' joint action $a^t = (a_i^t, a_{-i}^t)$ and their kinematic models, e.g. single track, applied for action duration τ_a to o^t . An index $-i$ indicates joint action of all agents except agent i . The process continues until some terminal criterion applies, e.g. collision or goal reached. Using this environment model we define a violation risk.

Definition 3.1: Violation risk: Given the current environment state $o^t \in \mathcal{O}$, behavior policies π_i and π_j , a safety violation indicator $f : \mathcal{O} \rightarrow \{0, 1\}$ indicating a safety violation in observation $o' \in \mathcal{O}$, then the violation risk is defined as:

$$\rho(o^t, \pi_i, \pi_j, f) = \mathbb{E}_{F_o \sim \mathbb{P}^{o^t, \pi_i, \pi_j}} \left[\frac{\sum_{z=1}^{|F_o|-1} f(F_o(z)) \cdot \tau_a}{|F_o| \cdot \tau_a} \right] \quad (1)$$

The expectation is defined over the distribution $\mathbb{P}^{o^t, \pi_i, \pi_j}$ over future observation sequences $F_o = (o^t, o^{t+\tau_a}, o^{t+2\tau_a}, \dots)$ starting from current environment state o^t . It is influenced by ego and other agents policies. The upper sum represents the violation duration within the observation sequence F_o with $|F_o|$ being the length of the sequence and $F_o(z)$ giving the z -th observation within the sequence. The lower term is the total duration of the sequence. The fraction of these terms yields the percentage of time the safety envelope is violated for one sequence. A sequence ends in a terminal state. The temporal resolution of this fraction is determined by the action duration τ_a . For fixed ego policy π_i , the expectation provides the *time-based* violation risk under unknown behavior of other participants π_j .

Using equation 1, we formalize risk-constrained interactive safety against behavior uncertainty.

Definition 3.2: Risk-constrained safety: Given an indicator function for safety envelope violations f_{envelope} , the behavior planner generates a goal-directed policy π_i in the

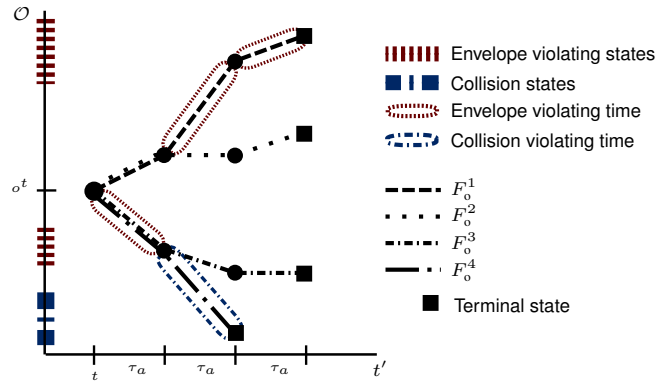


Fig. 2: Example for envelope violation and collision risk calculation: Four future observation sequences F_o^{1-4} starting from state o^t are sampled with probabilities $\mathbb{P}(F_o^{1-3}) = 0.3$ and $\mathbb{P}(F_o^4) = 0.1$, with F_o^4 ending due to a terminal collision state. Since sequence F_o^1 shows 2 and sequences F_o^{3-4} show 1 envelope violation, we obtain $\rho_{\text{env}}(\cdot) = 0.3 \cdot \frac{2\tau_a}{3\tau_a} + 0.3 \cdot \frac{0\tau_a}{3\tau_a} + 0.3 \cdot \frac{1\tau_a}{3\tau_a} + 0.1 \cdot \frac{1\tau_a}{2\tau_a} = 0.35$. The only sequence showing a collision violation is F_o^4 giving $\rho_{\text{col}}(\cdot) = 0.3 \cdot \frac{0\tau_a}{3\tau_a} + 0.3 \cdot \frac{0\tau_a}{3\tau_a} + 0.3 \cdot \frac{0\tau_a}{3\tau_a} + 0.1 \cdot \frac{1\tau_a}{2\tau_a} = 0.05$.

current environment state o^t under unknown behavior π_j of other participants which achieves a safety envelope violation risk lower than a specified allowed risk level β :

$$\rho(o^t, \pi_i, \pi_j, f_{\text{envelope}}) \stackrel{!}{\leq} \rho_{\text{env}}(o^t, \pi_i, \pi_j) \stackrel{!}{\leq} \beta \quad (2)$$

Our risk formulation is independent of the goal formalism, e.g. based on rewards, and the actual safety envelope definition e.g. being based on safe distance measures or reachability analysis. Since, the collision risk is difficult to interpret and infeasible to calculate exactly, we require it to be close to zero, $\rho(o^t, \pi_i, \pi_j, f_{\text{collision}}) \stackrel{!}{\approx} \rho_{\text{col}}(o^t, \pi_i, \pi_j) \stackrel{!}{\approx} 0$ with $f_{\text{collision}}$ denoting a collision indicator. Fig. 2 provides an example of envelope and collision risk calculations.

To satisfy our problem definition, the planner must correctly approximate the observation sequence distribution under unknown behavior of other agents and optimize a multi-objective criterion integrating the safety envelope and collision risk constraints and the goal-directed optimality criterion. In the next section, we propose a game-theoretic model, the RC-RSBG and a variant of MA-MCTS to solve the defined problem.

IV. RISK-CONSTRAINED INTERACTIVE PLANNING

We present a game-theoretic model, the Risk-Constrained Robust Stochastic Bayesian Game (RC-RSBG), which combines

- the RSBG presented by Bernhard *et al.* [6] to approximate the observation sequence distribution in eq. 1 given unknown behavior of other participants π_j
- and the Cost-Constrained Partially Observable Markov Decision Process (CC-POMDP) to incorporate risk constraints,
- and adapt a MA-MCTS planner to solve the RC-RSBG.

We detail each of these aspects in the following.

A. Robust Stochastic Bayesian Game (RSBG)

In Bernhard *et al.* [6], the authors presented the Robust Stochastic Bayesian Game (RSBG), a game-theoretic model for interactive planning to cover the *physically* feasible *continuous* variations inherent to human behavior considering both inter-driver and intra-driver variabilities [34]. The model uses a predefined set of hypothetical behavior types $\theta^k \in \Theta$ and behavior hypotheses $a_j^t \sim \pi_{\theta^k}(a_j^t|H_0^t)$. To predict the others' behavior one tracks the posterior beliefs $\Pr(\theta^k|H_0^t, j)$ over hypothesized types for each agent based on the action-observation history $H_0^t \in \mathcal{H}_0$.

To obtain behavior types and hypothesis, it defines a hypothetical policy

$$\pi^* : \mathcal{H}_0 \times \mathcal{B}_j^t \rightarrow A_j \quad (3)$$

for a specific task with $b_j^t \in \mathcal{B}_j^t$ being j th agent's behavior state at time t , $\mathcal{B}_j^t \subset \mathbb{R}^{N_B}$ its behavior space of dimension N_B . A behavior state b_j^t is a *physically interpretable* quantity describing j th continuous behavior variations. The other agents' behavior spaces \mathcal{B}_j^t and their current behavior states b_j^t are unknown. By using the property of physical interpretability of b_j^t , an expert can define a hypothesized behavior space \mathcal{B} , comprising the individual behavior spaces \mathcal{B}_j ($\mathcal{B}_j \subset \mathcal{B}$), by looking at the physically realistic situations. For instance, it is straightforward to define the physical boundaries of a behavior state modeling the desired gap between vehicles j and i at the time point of merging onto another lane with the one-dimensional behavior space $\mathcal{B} = \{b|b \in [0, d_{\max}]\}$ where d_{\max} is the maximum sensor range. The approach then uses a partitioning of the full behavior space $\mathcal{B} = \mathcal{B}^1 \cup \mathcal{B}^2 \cup \dots \cup \mathcal{B}^K$, $\forall l \neq k: \mathcal{B}^l \cap \mathcal{B}^k = \emptyset$. This yields K hypothesis π_{θ^k} by adopting a uniform distribution over behavior states within behavior space partitions \mathcal{B}^k , respectively.

The RSBG computes an optimal ego policy integrating the current posterior type belief $\Pr(\theta^k|H_0^t, j)$ according to $\pi_i = \max_{\pi_i} Q^{\pi_i}(H_0^t)$, where $Q^{\pi_i}(H_0^t) =$

$$\mathbb{E}_{\pi_i, (\theta_j^k, \dots)_{\forall j} \sim \Pr(\cdot|H_0^t, j)} \left[\sum_{t'=t}^{\infty} \gamma^{t'} r(o^{t'}, a^{t'}) \right] \quad (4)$$

with $a^{t'} = (a_i^{t'}, a_{-i}^{t'})$,
 $a_i^{t'} \sim \pi_i(\cdot|o^{t'})$,
 $a_{-i}^{t'} = (a_j^{t'}, \dots)_{\forall j} \sim \pi_{\theta^k}$

is the expected cumulative reward of agent i in state o^t and history H_0^t . Future rewards $r(o^t, a^t)$ are discounted by γ . We denote independent sampling from P and sample concatenation for all other agents j with $(\cdot, \dots)_{\forall j} \sim P$.

B. Risk-Constrained Robust Stochastic Bayesian Game

Next, we integrate the risk constraints for safety envelope violation and collision into the RSBG. For this, we approximate the unknown behavior of other agents π_j in the constraint eq. 1 using a mixture distribution $\hat{\pi}_j$ combining

hypotheses and posterior beliefs for each other agent j :

$$\hat{\pi}_j(a_j|H_0^t) = \sum_{\forall k} \Pr(\theta^k|H_0^t, j) \cdot \pi_{\theta^k}(a_j|H_0^t) \quad (5)$$

Optimality of RC-RSBGs is then defined by extending eq. 4 with the risk constraints.

Definition 4.1: Optimality of RC-RSBGs The optimal ego policy π_i of the RC-RSBG maximizes the expected cumulative reward $Q^{\pi_i}(H_0^t)$ defined in eq. 4 subject to

$$\begin{aligned} \rho_{\text{env}}(o^t, \pi_i, \hat{\pi}_j) &\stackrel{!}{\leq} \beta \\ \rho_{\text{col}}(o^t, \pi_i, \hat{\pi}_j) &\stackrel{!}{\approx} 0 \end{aligned} \quad (6)$$

Next, we present a Multi-Agent Monte Carlo Tree Search (MA-MCTS) approach which solves the RC-RSBG.

C. Monte Carlo Tree Search for the RC-RSBG

Our MA-MCTS approach is shown in Alg. 1. To solve the RSBG, as presented in [6], we use:

- Stage-wise action selection: Similar to [2, 3] agents select actions independently in stages. Their joint action yields the next environment state. In contrast to previous work [2, 3], we define separate selection mechanisms for ego and other agents' in EGOACTIONSELECTION and OTHERACTIONSELECTION each returning actions a_i or a_j at stage nodes $\langle H_0 \rangle$. Ego actions are discrete. Other agents' actions are continuous and their selection strategy represents the agents' behavior types.
- Hypothesis-belief-sampling: At the beginning of each search iteration, we sample a hypothesis for each other agent j from the posterior belief $\theta_j^k \sim \Pr(\theta^k|H_0^t, j)$ and use it within the function OTHERACTIONSELECTION for selection, expansion and roll-out steps.

To extend the MA-MCTS approach to solve the RC-RSBG, we develop an ego action selection mechanism EGOACTIONSELECTION based on solutions to CC-POMDPs. The POMDP is a well known single-agent framework to model sequential decisions under partially observable environment states. An optimal policy of a Cost-Constrained Partially Observable Markov Decision Process (CC-POMDP) [29, 30] not only maximizes the expected cumulative reward but also constraints M expected cumulative costs $Q_{C_m} \leq \hat{c}_m$, $m \in M$.

Lee *et al.* [30] use Monte Carlo Tree Search (MCTS) to solve CC-POMDPs by reformulating the problem as an *unconstrained* POMDP. They introduce Lagrange multipliers and express the optimal value function as $Q_\lambda^* = Q_R - \sum_{\forall m} \lambda_m^* \cdot Q_{C_m}$ for optimal λ_m^* . A solution is found by updating the Lagrange multipliers iteratively at the beginning of each MCTS iteration using a gradient estimate $\Delta \lambda_m \sim Q_{C_m} - \hat{c}_m, \forall m$.

We adapt their approach to solve the RC-RSBG. Yet, instead of cumulative costs, we maintain ego envelope violation and collision action-risks $\rho_{\text{env}}(\langle H_0 \rangle, a_i)$ and $\rho_{\text{col}}(\langle H_0 \rangle, a_i)$ in each stage node. For this, we separately backpropagate the violation durations for safety envelope T_{env} and collision T_{col} , and total time T_{tot} occurred with

Algorithm 1: Multi-Agent Monte Carlo Tree Search for the Risk-Constrained Robust Stochastic Bayesian Game

```

function SEARCH( $o^t, \Pr(\theta^k | H_0^t, \cdot)$ )
   $\lambda \leftarrow \text{RANDOMINIT}()$ 
  repeat
    for  $j = 1 \dots N_j$  do
       $\theta_j^t \sim \Pr(\theta^k | H_0^t, j)$ 
      SIMULATE( $\langle o^t \rangle, \theta_j^t \forall j, 1$ )
       $a_i \sim \text{EGOACTIONSELECTION}(\langle o^t \rangle, 0)$ 
       $\lambda_{\text{env}} \leftarrow \lambda_{\text{env}} + \alpha_n [\rho_{\text{env}}(\langle o^t \rangle, a_i) - \beta]$ 
       $\lambda_{\text{col}} \leftarrow \lambda_{\text{col}} + \alpha_n [\rho_{\text{col}}(\langle o^t \rangle, a_i) - 0]$ 
      Clip  $\lambda_{\text{env}}, \lambda_{\text{col}}$  to range  $[0, 1]$ 
  until MAXITERATIONS()
  return EGOACTIONSELECTION( $\langle o^t \rangle, 0$ )

function OTHERACTIONSELECTION( $\langle H_0 \rangle, j, \theta_j$ )
  if PROGRESSIVEWIDENING() then
    return  $a_j \leftarrow \pi_{\theta_j}(a_j | H_0)$ 
  else
    return  $\text{argmax}_a Q_{\overline{C}}(\langle H_0 \rangle, a_j, j)$ 

function EGOACTIONSELECTION( $\langle H_0 \rangle, \kappa$ )
   $Q_{\lambda}^{\oplus}(\langle H_0 \rangle, a) \leftarrow Q_R(\langle H_0 \rangle, a) - \lambda_{\text{env}} \cdot \rho_{\text{env}}(\langle H_0 \rangle, a)$ 
   $\quad - \lambda_{\text{col}} \cdot \rho_{\text{col}}(\langle H_0 \rangle, a) + \kappa \sqrt{\log N(\langle H_0 \rangle) / N(\langle H_0 \rangle, a, i)}$ 

   $a^* \leftarrow \text{argmax}_a Q_{\lambda}^{\oplus}(\langle H_0 \rangle, a)$ 
   $A^* \leftarrow$  add other actions to  $a^*$  to consider exploration differences
   $\pi_i \leftarrow$  Solve linear program with  $A^*$  to obtain stochastic policy
  return  $a_i \sim \pi_i$ 

function SIMULATE( $\langle H_0 \rangle, \theta_j^t \forall j, d$ )
  if  $d > d_{\text{max}}$  or ISTERMINAL( $\langle H_0 \rangle$ ) then
    return  $[0, 0, 0, 0]$ 
  if FIRSTNODEVISIT( $\langle H_0 \rangle$ ) then
    return RANDOMROLLOUT( $\langle H_0 \rangle, \theta_j^t \forall j, d$ )
   $a_i \leftarrow \text{EGOACTIONSELECTION}(\langle H_0 \rangle, \kappa)$ 
  for  $l = 1 \dots N_j$  do
     $a_{jl} \leftarrow \text{OTHERACTIONSELECTION}(\langle H_0 \rangle, l, \theta_l^t)$ 
   $\tau_{\text{predict}} \leftarrow d \cdot \tau_a$ 
   $(o', r) \leftarrow \text{ENVIRONMENTMOVE}(H_0, (a_i, a_j), \tau_{\text{predict}})$ 
   $[R', T'_{\text{env}}, T'_{\text{col}}, T'_{\text{tot}}, \overline{C}'] \leftarrow \text{SIMULATE}(\langle H_0 \rangle, (a_i, a_j), o', \theta_j^t \forall j, d + 1)$ 
   $[R, T_{\text{env}}, T_{\text{col}}, T_{\text{tot}}] \leftarrow [r + \gamma \cdot R', T'_{\text{env}} + f_{\text{envelope}}(o') \cdot \tau_{\text{predict}},$ 
   $\quad T'_{\text{col}} + f_{\text{collision}}(o') \cdot \tau_{\text{predict}}, T'_{\text{tot}} + \tau_{\text{predict}}]$ 
   $N(\langle H_0 \rangle) \leftarrow N(\langle H_0 \rangle) + 1$ 
   $N(\langle H_0 \rangle, a_i, i) \leftarrow N(\langle H_0 \rangle, a_i, i) + 1$ 
   $Q_R(\langle H_0 \rangle, a_i) \leftarrow Q_R(\langle H_0 \rangle, a_i) + (R - Q_R(\langle H_0 \rangle, a_i)) / N(\langle H_0 \rangle, a_i, i)$ 
   $\rho_{\text{env}}(\langle H_0 \rangle, a_i) \leftarrow \rho_{\text{env}}(\langle H_0 \rangle, a_i) + (T'_{\text{env}} / T_{\text{tot}} - \rho_{\text{env}}(\langle H_0 \rangle, a_i)) / N(\langle H_0 \rangle, a_i, i)$ 
   $\rho_{\text{col}}(\langle H_0 \rangle, a_i) \leftarrow \rho_{\text{col}}(\langle H_0 \rangle, a_i) + (T'_{\text{col}} / T_{\text{tot}} - \rho_{\text{col}}(\langle H_0 \rangle, a_i)) / N(\langle H_0 \rangle, a_i, i)$ 
  for  $l = 1 \dots N_j$  do
     $N(\langle H_0 \rangle, a_{jl}, l) \leftarrow N(\langle H_0 \rangle, a_{jl}, l) + 1$ 
     $\overline{C} \leftarrow f_{\text{envelope}}(o') + f_{\text{collision}}(o') + \gamma \cdot \overline{C}'$ 
     $Q_{\overline{C}}(\langle H_0 \rangle, a_{jl}, l) \leftarrow Q_{\overline{C}}(\langle H_0 \rangle, a_{jl}, l) + (\overline{C} - Q_{\overline{C}}(\langle H_0 \rangle, a_{jl}, l)) / N(\langle H_0 \rangle, a_{jl}, l)$ 
  return  $[R, T_{\text{env}}, T_{\text{col}}, T_{\text{tot}}, \overline{C}]$ 

```

this iteration's selection, expansion and rollout step in the SIMULATE() function. These terms correspond to the upper and lower term of the ratio defined in eq. 1 and can be used to update $\rho_{\text{env}}(\langle H_0 \rangle)$ and $\rho_{\text{col}}(\langle H_0 \rangle)$ in each iteration. Return estimates are updated as usual. Prediction time τ_{predict} increases with search depth d .

In the search method, we perform a gradient update of the Lagrange multipliers λ_{env} and λ_{col} using the root node's risks estimates $\rho_{\text{env}}(\langle o^t \rangle, a_i)$ and $\rho_{\text{col}}(\langle o^t \rangle, a_i)$ and desired risk constraints β and 0 with decreasing step size $\alpha_n \sim 1/\text{NUMITERATIONS}()$. In EGOACTIONSELECTION, we calculate the combined action-value based on the estimated Lagrange multipliers. As proposed in [30], we account for inaccuracies in return and risk estimates and form a set of equal-valued actions A^* maximizing the action-value by accepting a tolerance based on action selection counts. An optimal policy of a CC-POMDP is generally stochastic. In our case, this requires

$$\begin{aligned}
 \sum_{a_i \in A^*} \pi_i(a_i | o^t) \cdot \rho_{\text{env}}(\langle o^t \rangle, a_i) &\stackrel{!}{\leq} \beta \\
 \sum_{a_i \in A^*} \pi_i(a_i | o^t) \cdot \rho_{\text{col}}(\langle o^t \rangle, a_i) &\stackrel{!}{=} 0
 \end{aligned} \tag{7}$$

We solve the linear program defined in [30] to obtain a stochastic policy π_i satisfying eq. 7, 4 and 6.

We apply worst-case action selection in combination with progressive widening for other agents in OTHERACTIONSELECTION. Other agents maintain separate *combined* ego cost estimates $Q_{\overline{C}}(\langle H_0 \rangle, a_j, j)$ during back-propagation for their own selected actions. Progressive widening ensures that new actions are explored. In the other case, other agents select actions *maximizing* the combined envelope violation

and collision cost of the ego agent. As shown in [6], this concept reduces sample complexity when other agents select actions from a continuous action space. In the case of a constrained setting, it additionally improves convergence by better exploring joint actions which violate the given risk constraints.

V. EXPERIMENT

In our experiment, we evaluate quantitatively over many driven scenarios with simulated behavior uncertainty

- if the presented planning approach respects the specified risk level β ,
- how the risk parameter β balances safety and efficiency,
- and how our approach compares against baseline interactive planners.

We also qualitatively analyze the computed policy and posterior beliefs in specific scenarios.

A. Scenarios

We use the OpenSource behavior benchmarking environment BARK [24] for simulating two dense traffic scenarios:

- Freeway enter: In a double merge, the ego vehicle wants to enter the freeway on the left occupied lane.
- Left turn: The ego vehicle wants to turn left from a side into a main road having to cross two occupied lanes.

We uniformly sample initial starting conditions, e.g. the distances between vehicles from $[15\text{m}, 30\text{m}]$ and velocities from $[\frac{30}{3.6} \frac{\text{m}}{\text{s}}, \frac{50}{3.6} \frac{\text{m}}{\text{s}}]$. Fig. 3 provides examples of the scenarios. A scenario successfully terminates when the ego vehicle is close to and oriented towards the goal while the velocity is within the sampling bounds.

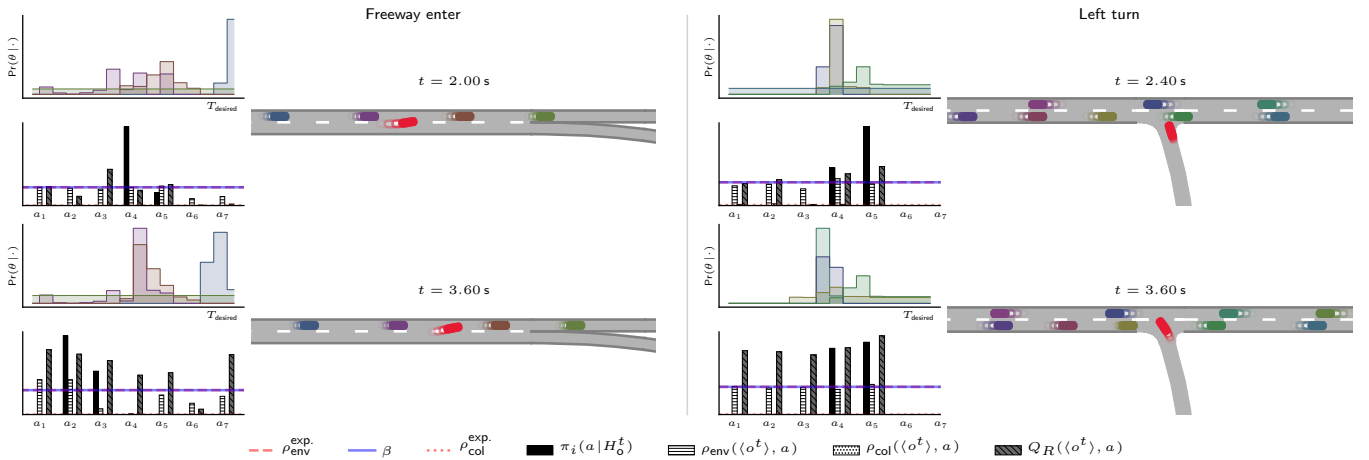


Fig. 3: Scenario analysis at two time steps with posterior beliefs $\Pr(\theta^k | H_0^t, j)$ for four nearest agents in respective color. The planned stochastic policy π_i balances action-risk estimates, $\rho_{\text{env}}(\langle o^t \rangle, a_i)$ and $\rho_{\text{col}}(\langle o^t \rangle, a_i)$ yielding an expected envelope risk $\rho_{\text{env}}^{\text{exp}}$ fulfilling the risk constraint $\beta = 0.2$ while the expected planned collision risk $\rho_{\text{col}}^{\text{exp}}$ is close to zero and higher returns $Q_R(\langle H_0 \rangle, a_i)$ are preferred.

B. Behavior Simulation & Space

The Intelligent Driver Model (IDM) [34] defines both the simulated unknown behavior π_j of other participants and hypothetical policy π^* used for hypotheses design. For simulation, we define a 5-dimensional true behavior space \mathcal{B}_{5D}^* over the IDM parameters and uniformly draw unknown boundaries of behavior variations $[b_{j,\min}^l, b_{j,\max}^l]$, $l \in \{1, \dots, 5\}$ for each agent and trial ($\mathcal{B}_j \subseteq \mathcal{B}_{5D}^*$). We introduce the parameters minimum and maximum boundary widths $\Delta_{\min}/\Delta_{\max}$ to specify minimum and maximum time-dependent variations of behavior states in simulation. This avoids unrealistic large variations of behavior parameters.

For hypotheses design, we employ a 1D-behavior space, since, as shown in [6], lower-dimensional behavior spaces can capture the uncertainty occurring with the 5-dimensional true behavior space. Tab. I depicts both the simulated 5D and hypothesized 1-D behavior space used in our experiment.

We simulate the other agents by sampling a new behavior state b_j^t at every time step from the unknown boundaries of behavior variations \mathcal{B}_j and then use the IDM model with this parameters to choose their actions. Fixing the random seeds for all sampling operations ensures equal conditions for all evaluations.

C. Safety Violation Indicators

Rizaldi *et al.* [35] propose a model for longitudinal safe distances between vehicles which we use to define the indicator f_{envelope} to return a violation if the ego vehicle violates the safe distance to other vehicles. The response

Param b^l	\mathcal{B}_{5D}^*		$\mathcal{B}_{1D,\text{Head}}$
	$[b_{\min}^l, b_{\max}^l]$	$\Delta_{\min}/\Delta_{\max}$	$[b_{\min}^l, b_{\max}^l]$
v_{desired} [m/s]	[8.0, 14.0]	0.1 / 0.1	11.0
T_{desired} [s]	[0.5, 2.0]	0.1 / 0.3	[0.0, 4.0]
s_{\min} [l]	[2.0, 2.5]	0.1 / 0.3	2.25
\dot{v}_{factor} [m/s ²]	[11.5, 2.0]	0.1 / 0.3	1.75
\dot{v}_{comft} [m/s ²]	[1.7, 2.0]	0.1 / 0.3	1.85

TABLE I: Boundaries of the simulated true behavior spaces \mathcal{B}_{5D}^* and the hypothesized behavior space $\mathcal{B}_{1D,\text{Head}}$ for IDM parameters desired velocity v_{desired} , desired time headway T_{desired} , minimum spacing s_{\min} , acceleration factor \dot{v}_{factor} , comfortable braking \dot{v}_{comft} .

time of other vehicles is 1 s. For the ego vehicle, we use 0.5 s in freeway and, due to higher traffic density, 1 s in left turn. The deceleration limit is $-5 \frac{\text{m}}{\text{s}^2}$ as in the IDM model.

The indicator $f_{\text{collision}}$ indicates a collision when another vehicle overlaps with a static safety boundary of 0.5 m around the ego vehicle. We introduce a static safety boundary instead of using the exact geometric collision check to account for potential inaccuracy due to sampling with MCTS approaches.

D. Planning Algorithms

We compare the **RC-RSBG** and the variant **RC-RSBGFullInfo** which employs the true simulated behavior policies π_j for prediction to several baseline algorithms. We focus on interactive planners suitable for dense traffic. RC-RSBG and RC-RSBGFullInfo use a simplistic reward function $r(\cdot) = 1.0 \cdot \text{GOAL REACHED}(\cdot)$. To model risk-awareness with the single-objective baselines, we define the reward function $r(\cdot) = 0.1 \cdot \text{GOAL REACHED}(\cdot) - 0.1 \frac{f_{\text{envelope}}(\cdot) \cdot \tau_{\text{predict}}}{\beta \cdot T_{\text{Plan}}} - 1.0 f_{\text{collision}}(\cdot)$. It is designed such that it fully erases the goal reward when the predicted envelope violation duration $\sum_{\forall t'} f_{\text{envelope}}(\cdot) \tau_{\text{predict}}$, exceeds the allowed duration $\beta \cdot T_{\text{Plan}}$ with T_{Plan} being the maximum planning horizon. Using this reward function, we define the following baselines

- **RSBG** uses a MA-MCTS with hypothesis-based prediction and reward-based worst-case action selection for other agents,
- **MDP** does not incorporate belief information over hypotheses. Instead it predicts other participants by sampling behavior states from the full hypothesized behavior space $\mathcal{B}_{1D,\text{Head}}$,
- **Cooperative** does not use the behavior space model for prediction. In its MA-MCTS, other agents select actions based on a global cost function which weights subjective and others' rewards based on a cooperation factor $c = 0.1$ after evaluating $r(\cdot)$ for each agent.

All baselines use an Upper Confidence Bound (UCB) action selection strategy for the ego agent, the cooperative approach additionally for the other agents. All plan-

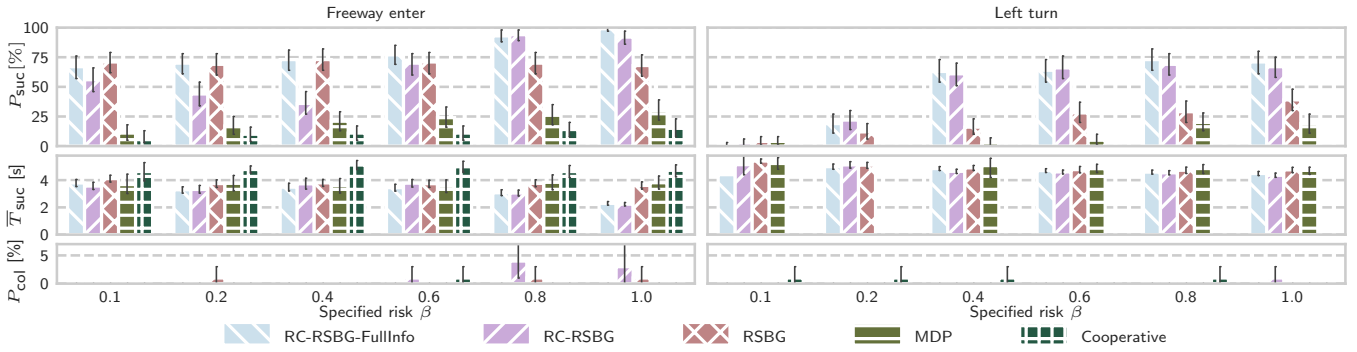


Fig. 4: Performance metrics for **RC-RSBG** planner and baselines for increasing envelope violation risk levels β .

ners use an equal ego action space consisting of the macro actions lane changing, lane keeping at constant accelerations, $\dot{v}_i = \{-5, -1, -2, 1, 2\} [\text{m/s}^2]$ for freeway and $\dot{v}_i = \{-5, -1, 0, 1, 2\} [\text{m/s}^2]$ for left turn, and gap keeping based on the IDM for freeway. The cooperative approach employs this action space additionally for the other agents. All planners use $\tau_a = 0.2 \text{ s}$, a max search depth $d_{\max} = 10$ yielding $T_{\text{plan}} = 11 \text{ s}$. We obtain $K = 16$ hypothesis π_{θ^k} , $k \in \{1, \dots, K\}$ by equally partitioning the hypothesized behavior space $\mathcal{B}_{1D, \text{Head}}$. In this work, the focus is on evaluating the proposed risk formulation and decision model, the **RC-RSBG**, and not on working towards real-time capability with MA-MCTS. All planners use an equal number of 20000 iterations to minimize influence of sampling inaccuracies.

E. Results

First, we *qualitatively* analyze the **RC-RSBG** planner in Fig. 3 for two time steps in each scenario. The ego vehicle is shown in red. The posterior beliefs $\Pr(\theta^k | H_0^t, j)$ given for the four nearest other vehicles in the respective color qualitatively reflect the desired distance to the respective leading agent. The posterior is uniformly distributed for vehicles without a leading vehicle. We see that the planned stochastic policy π_i correctly balances envelope and collision action-risk estimates, $\rho_{\text{env}}(\langle H_0^t \rangle, a_i)$ and $\rho_{\text{col}}(\langle H_0^t \rangle, a_i)$ such that the expected planned envelope risk $\rho_{\text{env}}^{\text{exp.}}$ (dashed red) fulfills the constraint $\beta = 0.2$ (blue) while the expected planned collision risk $\rho_{\text{col}}^{\text{exp.}}$ (dotted red) is close to zero. Given these constraints, the planned policy prefers actions with higher expected action-return values $Q_R(\langle H_0 \rangle, a_i)$. Our qualitative analysis reveals that the **RC-RSBG** planner correctly implements the risk-constrained optimality criteria from Sec. IV-B using a stochastic policy.

Next, we *quantitatively* analyze the percentage of trials

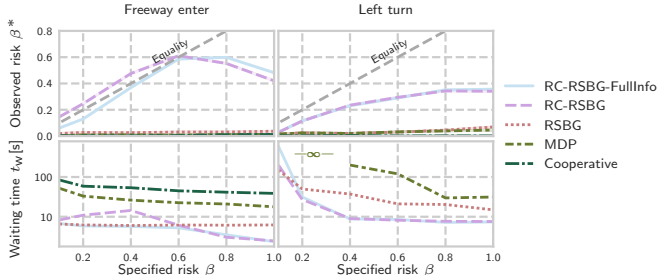


Fig. 5: Analysis of observed envelope violation risk β^* and expected scenario waiting time t_w for different risk levels β .

over 100 scenarios where the ego vehicle reaches the goal P_{suc} , collides P_{col} or exceeds the maximum allowed simulation time, P_{\max} to solve a scenario ($t \leq 6.0 \text{ [s]}$). We evaluate over increasing envelope risk constraint β . For successful trials, we calculate the average time to reach the goal \bar{T}_{suc} . Results are given in Fig. 4. The **RC-RSBG** planner outperforms the baselines with increasing β regarding P_{suc} and \bar{T}_{suc} . The **MDP** and **Cooperative** planner do rarely succeed ($P_{\text{suc}} \ll 25\%$) emphasizing the advantage of belief-based prediction in denser traffic. With higher β the **RC-RSBG** planner increasingly relies on the accuracy of the prediction model, and lesser on the safety provided by the envelope restriction. In the case of prediction model inaccuracies this provokes collisions for $\beta \geq 0.6$. This tendency is not observed with baseline planners which show collisions also for lower β . The **RC-RSBG-FullInfo** planner having access to the true behavior of other vehicles does not suffer from model inaccuracies, and, thus does not provoke any collision. These findings indicate the usefulness of multi-objective optimality to integrate risk constraints, and support our problem formulation considering risk to balance prediction model inaccuracies and safety, as discussed in Sec. III.

To further analyze how β balances safety and efficiency, we introduce two metrics, the observed envelope violation risk β^* and the expected scenario waiting time t_w . The observed envelope violation risk is the percentage of simulation time the envelope is violated, $\beta^* = \frac{\sum_{\forall f} \sum_{o^t \in f} f_{\text{envelope}}(o^t) \cdot \tau_a}{\sum_{\forall f} L(f) \cdot \tau_a}$ with $o^t \in f$ giving the simulated states and $L(f)$ the length of the scenario f . The expected waiting time, $\bar{t}_w = \sum_{k=0}^{\infty} (\bar{T}_{\max} k + \bar{T}_{\text{suc}}) \cdot (P_{\text{suc}} P_{\max}^k)$ defines the expected time to solve a scenario. The calculation assumes that the ego vehicle encounters solvable scenarios with probability P_{suc} and duration \bar{T}_{suc} and unsolvable scenarios with probability P_{\max} with duration equal to the allowed simulation time $\bar{T}_{\max} = 6 \text{ s}$. Fig. 5 shows both metrics over risk level β . In scenario freeway enter, the **RC-RSBG** planners fully exploit the allowed risk ($\beta^* \approx \beta$) for $\beta < 0.8$, indicating that our *risk formulation and planning approach reflects the observed risk*. For $\beta \geq 0.8$, β^* decreases. We assume that the scenario ending becomes less risky by allowing higher β initially. The opposite case occurs in the left turn scenario where a low β prevents entering the intersection impeding full exploitation of allowed β . The baseline approaches do not show any interpretable correlation between β^* and β . The waiting time

t_w indicates efficiency while P_{col} from Fig. 4 defines safety. Interestingly, our risk formulation suggests $\beta \leq 0.4$ in the freeway enter scenario to prevent collisions which resembles the safety envelope violation risk of humans during lane changing, $\beta_{\text{human}} \approx 10\% - 40\%$ [12, 13] and introduces a natural trade off between safety and efficiency for $\beta > 0.4$. With our risk formulation waiting times are within a realistic human-like range, $t_w \approx 2\text{ s} \dots 15\text{ s}$ in dense traffic whereas the baseline approaches show mostly larger waiting times.

We conclude, that the presented risk formulation and interactive planner balances safety and efficiency according to human-related risk criteria in dense traffic. It outperforms interactive baseline planners regarding efficiency and interpretability of their employed safety objectives.

VI. CONCLUSION

This work formalizes a novel safety objective for interactive planning which balances safety and efficiency in dense traffic scenarios with uncertainty about other traffic participants' behavior by accepting a specifiable risk of violating a safety envelope. We propose a decision-theoretic framework under this safety objective, the Risk-Constrained Robust Stochastic Bayesian Game (RC-RSBG), and an accompanying interactive planner based on a variant of Multi-Agent Monte Carlo Tree Search. In two types of traffic scenarios, we demonstrate that the RC-RSBG planner outperforms baseline planners and provides an interpretable and tunable safety objective.

This work reveals that a combination of uncertainty- and prediction based interactive planners with safety envelope restrictions is a promising direction for future research. We will further invest into the real-time capability of the planner, improve safety envelope definitions, and analyze in detail the correspondence between human risk concepts and the proposed risk level formalism.

VII. ACKNOWLEDGEMENT

This research was funded by the Bavarian Ministry of Economic Affairs, Regional Development and Energy, project Dependable AI.

REFERENCES

- [1] Y. Wang *et al.*, "Enabling courteous vehicle interactions through game-based and dynamics-aware intent inference," *IEEE Transactions on Intelligent Vehicles*, vol. 5, no. 2, 2020.
- [2] D. Lenz *et al.*, "Tactical cooperative planning for autonomous highway driving using Monte-Carlo Tree Search," in *Intelligent Vehicles Symposium (IV)*, IEEE, 2016.
- [3] K. Kurzer *et al.*, "Decentralized Cooperative Planning for Automated Vehicles with Hierarchical Monte Carlo Tree Search," in *Intelligent Vehicles Symposium (IV)*, Jun. 2018.
- [4] C. Hubmann *et al.*, "A Belief State Planner for Interactive Merge Maneuvers in Congested Traffic," in *21st International Conference on Intelligent Transportation Systems (ITSC)*, IEEE, 2018.
- [5] Y. Lu *et al.*, "Safe mission planning under dynamical uncertainties," in *IEEE International Conference on Robotics and Automation (ICRA)*, 2020.
- [6] J. Bernhard *et al.*, "Robust Stochastic Bayesian Games for Behavior Space Coverage," in *Robotics: Science and Systems (RSS), Workshop on Interaction and Decision-Making in Autonomous-Driving*, 2020.

- [7] C. Pek *et al.*, "Using online verification to prevent autonomous vehicles from causing accidents," *Nature Machine Intelligence*, vol. 2, Sep. 2020.
- [8] K. Leung *et al.*, "On infusing reachability-based safety assurance within planning frameworks for human-robot vehicle interactions," *International Journal of Robotics Research*, vol. 39, no. 10-11, 2020.
- [9] M. -Y. Yu *et al.*, "Risk assessment and planning with bidirectional reachability for autonomous driving," in *2020 IEEE International Conference on Robotics and Automation (ICRA)*, 2020.
- [10] S. Shalev-Shwartz *et al.*, "On a Formal Model of Safe and Scalable Self-driving Cars," 2017. arXiv: 1708.06374.
- [11] A. Pierson *et al.*, "Learning risk level set parameters from data sets for safer driving," in *2019 IEEE Intelligent Vehicles Symposium (IV)*, 2019.
- [12] K. Esterle *et al.*, "Formalizing traffic rules for machine interpretability," 2020. arXiv: 2007.00330.
- [13] C. Pek *et al.*, "Verifying the safety of lane change maneuvers of self-driving vehicles based on formalized traffic rules," in *2017 IEEE Intelligent Vehicles Symposium (IV)*, 2017.
- [14] C. Wei *et al.*, "Risk-based autonomous vehicle motion control with considering human driver's behaviour," *Transportation Research Part C: Emerging Technologies*, vol. 107, 2019.
- [15] D. Iberraken *et al.*, "Safe autonomous overtaking maneuver based on inter-vehicular distance prediction and multi-level bayesian decision-making," in *2018 21st International Conference on Intelligent Transportation Systems (ITSC)*, 2018.
- [16] Y. Akagi *et al.*, "Stochastic driver speed control behavior modeling in urban intersections using risk potential-based motion planning framework," in *2015 IEEE Intelligent Vehicles Symposium (IV)*, Jun. 2015.
- [17] C. M. Hruschka *et al.*, "Uncertainty-adaptive, risk based motion planning in automated driving," in *2019 IEEE International Conference on Vehicular Electronics and Safety (ICVES)*, 2019.
- [18] X. Huang *et al.*, "Hybrid Risk-Aware Conditional Planning with Applications in Autonomous Vehicles," in *2018 IEEE Conference on Decision and Control (CDC)*, Dec. 2018.
- [19] M. Yu *et al.*, "Occlusion-aware risk assessment for autonomous driving in urban environments," *IEEE Robotics and Automation Letters*, vol. 4, no. 2, 2019.
- [20] A. Philipp *et al.*, "Analytic collision risk calculation for autonomous vehicle navigation," in *2019 International Conference on Robotics and Automation (ICRA)*, 2019.
- [21] A. Majumdar *et al.*, "How Should a Robot Assess Risk? Towards an Axiomatic Theory of Risk in Robotics," *CoRR*, vol. abs/1710.11040, 2017.
- [22] J. Bernhard *et al.*, "Addressing Inherent Uncertainty: Risk-Sensitive Behavior Generation for Automated Driving using Distributional Reinforcement Learning," in *2019 IEEE Intelligent Vehicles Symposium (IV)*, IEEE, 2019.
- [23] J. I. Ge *et al.*, "Risk-aware motion planning for automated vehicle among human-driven cars," in *2019 American Control Conference (ACC)*, 2019.
- [24] J. Bernhard *et al.*, "BARK: Open behavior benchmarking in multi-agent environments," in *2020 IEEE/RSJ International Conference on Intelligent Robots and Systems (IROS)*, 2020.
- [25] W. Schwarting *et al.*, "Planning and Decision-Making for Autonomous Vehicles," in *Annual Review of Control, Robotics, and Autonomous Systems*, vol. 1, no. 1, May 2018.
- [26] M. Bouton *et al.*, "Reinforcement learning with probabilistic guarantees for autonomous driving," in *Workshop on Safety, Risk and Uncertainty in Reinforcement Learning, Conference on Uncertainty in Artificial Intelligence (UAI)*, 2018.
- [27] H. Bai *et al.*, "Intention-aware online POMDP planning for autonomous driving in a crowd," in *IEEE International Conference on Robotics and Automation (ICRA)*, IEEE, 2015.
- [28] M. Bouton *et al.*, "Belief state planning for autonomously navigating urban intersections," in *Intelligent Vehicles Symposium (IV)*, IEEE, 2017.
- [29] J. D. Isom *et al.*, "Piecewise linear dynamic programming for constrained POMDPs," in *Proceedings of the 23rd National Conference on Artificial Intelligence - Volume 1*, AAAI Press, 2008.
- [30] J. Lee *et al.*, "Monte-Carlo Tree Search for Constrained POMDPs," in *Advances in Neural Information Processing Systems 31*, Curran Associates, Inc., 2018.

- [31] J. Zhou *et al.*, "Gap acceptance based safety assessment of autonomous overtaking function," in *2019 IEEE Intelligent Vehicles Symposium (IV)*, 2019.
- [32] J. Müller *et al.*, "A risk and comfort optimizing motion planning scheme for merging scenarios*," in *2019 IEEE Intelligent Transportation Systems Conference (ITSC)*, 2019.
- [33] S. V. Albrecht *et al.*, "Belief and Truth in Hypothesised Behaviours," in *Artificial Intelligence*, vol. 235, Jun. 2016.
- [34] A. M. Uhrmacher *et al.*, *Multi-Agent Systems: Simulation and Applications*, 1st. CRC Press, Inc., 2009.
- [35] A. Rizaldi *et al.*, "Formalising and monitoring traffic rules for autonomous vehicles in Isabelle/HOL," in *Integrated Formal Methods*, Springer International Publishing, 2017.